

Hybrid-aligned nematic liquid-crystal modulators fabricated on VLSI circuits

Jean-Jacques P. Drolet

Department of Electrical Engineering, California Institute of Technology, Pasadena, California 91125

Jay S. Patel*

Navesink Research and Engineering Center, Bell Communications Research, 331 Newman Springs Road, Red Bank, New Jersey 07701

Konstantinos G. Haritos, Weihua Xu, Axel Scherer, and Demetri Psaltis

Department of Electrical Engineering, California Institute of Technology, Pasadena, California 91125

Received June 8, 1995

A new method for fabricating analog light modulators on VLSI devices is described. The process is fully compatible with devices fabricated by commercial VLSI foundries, and the assembly of the modulator structures requires a small number of simple processing steps. The modulators are capable of analog amplitude or phase modulation and can operate at video rates and at low voltages (2.2 V). The modulation mechanism and the process yielding the modulator structures are described. Experimental data are presented. © 1995 Optical Society of America

The development of highly integrated spatial light modulators and smart pixel arrays based on VLSI circuitry and liquid-crystal devices has recently made significant progress.^{1,2} Although some early work was conducted with nematic liquid crystals,³ most current efforts involve ferroelectric chiral smectic C liquid crystals in the surface-stabilized geometry⁴⁻⁸ that provide fast switching at low voltages. We demonstrate an alternative modulator structure that employs nematic liquid crystals in the hybrid-aligned nematic (HAN) configuration, which provides analog amplitude or phase modulation of an incident monochromatic readout beam. Prototype modulators fabricated on commercially processed VLSI devices have contrast ratios in excess of 18:1 and can operate at video rates.

Surface-stabilized ferroelectric liquid-crystal modulators require a very small cell gap, of the order of 1–2 μm , in order to ensure bistability and to yield a zero-order half-wave plate in one of the two stable states. This small cell gap makes the device very sensitive to the surface topology of the VLSI die, and a planarization treatment is generally required for contrast and uniformity to be improved.² In the case of nematic liquid crystals with larger cell gaps, the topmost layer of the integrated circuit, which acts as a bottom substrate for the liquid-crystal cell, must provide strong anchoring of the neighboring nematic. Although various surface treatments can provide strong homogeneous alignment, the deposition of a silane compound inducing homeotropic alignment provides strong anchoring at the bottom substrate while requiring a minimum of postprocessing to be performed on the fabricated semiconductor die or wafer.

In HAN liquid-crystal modulators, one substrate (the cover plate) induces strong homogeneous alignment, whereas the other substrate causes strong homeotropic alignment. By virtue of bulk elasticity the orientation of the nematic director undergoes a

smooth rotation from one substrate to the other,⁹ causing a splay-bend conformation in the nematic film, as illustrated in Fig. 1. When no electric field is applied across the cell, the locally averaged orientation of the molecules varies smoothly from a vertical state on the surface of the die to a horizontal state close to the cover plate. Using the Frank elasticity theory, assuming strong anchoring at both substrates, and using the one-constant approximation ($K_1 \approx K_3$), we can show that the angle (in radians) between the nematic director and the vertical axis (perpendicular to the substrates), $\phi(z)$, is approximately a linear function of depth within the cell:

$$\phi(z) \approx \frac{\pi}{2d} \left(z + \frac{d}{2} \right). \quad (1)$$

Under these conditions, assuming illumination by a normally incident beam, the total one-way phase retardation between the two eigenmodes of the cell is

$$\Delta\phi \approx \frac{2\pi}{\lambda} n_o d \left(\frac{2}{\pi} \int_0^{\pi/2} \frac{d\phi}{\sqrt{1 - R \sin^2 \phi}} - 1 \right), \quad (2)$$

where $R \equiv 1 - n_o^2/n_e^2$; n_o and n_e are, respectively, the ordinary and extraordinary indices of refraction

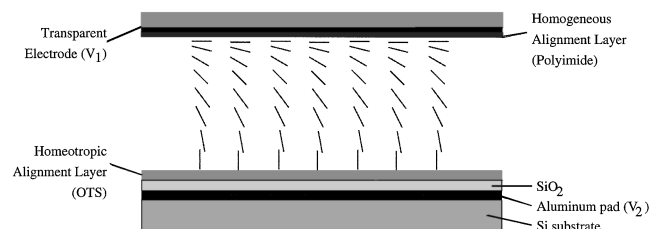


Fig. 1. Schematic of a reflective HAN cell fabricated on the surface of a VLSI die or wafer, showing the smoothly rotating director field.

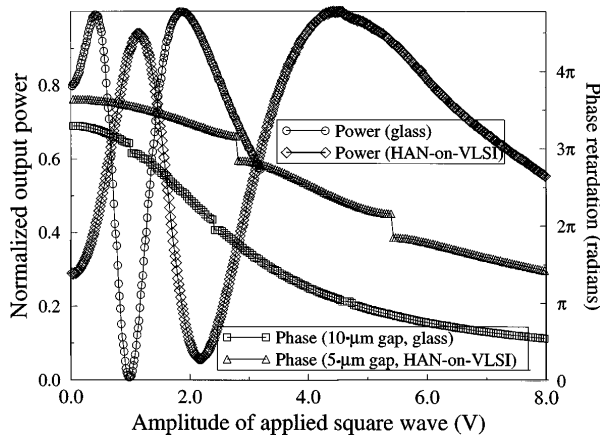


Fig. 2. Electro-optic characteristics at 632.8 nm of a transmissive HAN cell with a 10- μm gap and a reflective HAN-on-VLSI sample with a 5- μm gap. Both cells were filled with Merck E7. Note that the entire amplitude-modulation range of the HAN-on-VLSI device is spanned by the 1.1-V amplitude interval between 1.1 and 2.2 V.

of the uniaxial nematic liquid crystal; and λ is the wavelength of the incident optical beam in vacuum.

When an electric field is applied, the director tends to align with it. In the high-field limit, the director is perpendicular to the substrates throughout the cell, except for a thin film in the immediate vicinity of the cover plate, and there is practically no phase retardation between the eigenmodes of a normally incident plane wave. The effective index of refraction seen by light polarized along the buffing direction of the cover plate can be continuously changed by application of analog voltages across the cell. Given a suitable input light polarization, this phase modulation can be converted into amplitude modulation with the help of an analyzer.

The electro-optic response of a typical HAN sample is shown in Fig. 2 (curves labeled glass). The device, which had glass substrates and a cell gap of 10 μm , was filled with the nematic E7 from Merck, placed between crossed polarizers, illuminated by a collimated laser beam at 632.8 nm, and driven by a 1-kHz square wave of variable amplitude. The surface coupling agents inducing homogeneous and homeotropic alignment were buffed polyimide and octadecyltriethoxysilane (OTS), respectively. As expected, the transmission asymptotically goes to zero in the high-voltage regime, where the director (and hence the optic axis) is nearly normal to the substrates throughout the cell and the phase retardation between the eigenmodes excited by the normally incident beam is nearly zero. The phase retardation increases as the amplitude of the applied square wave decreases, until it reaches a maximum value determined by the cell gap, the properties of the nematic (indices of refraction, elastic constants), and the anchoring strength at the substrates. The phase retardation of the undriven device is seen to be 3.3 rad, in excellent agreement with the value (3.4 rad) predicted by relation (2), with the appropriate indices of refraction,¹⁰ $n_o = 1.5211$ and $n_e = 1.7464$, and assuming strong anchoring at both substrates. Note

that unlike parallel-rubbed cells, HAN devices have no threshold voltage for the onset of an electro-optic response.

We have also fabricated reflective HAN modulators on semiconductor dies processed by commercial foundries. In particular, our fabrication method is compatible with the Orbit Semiconductor 2.0- μm silicon-gate complementary metal-oxide-semiconductor process available through MOSIS.¹¹

Figure 1 schematically shows the cross section of a HAN-on-VLSI device. Metal electrodes made of one of the metalization levels provided by the semiconductor process are used to apply voltages locally across the liquid-crystal cell and as optical mirrors. They are overlaid by a silicon dioxide protective overcoat, which is also a native layer of the VLSI process and which helps OTS, the surface coupling agent inducing homeotropic alignment in the nematic film, to bind to the surface of the die. An OTS solution (2% mass in ethanol) is spun onto the VLSI die or wafer at 3000 rpm for 40 s and then baked at 200 $^{\circ}\text{C}$ for 30 min. This low-temperature operation does not affect the performance of the electronic circuitry. The glass cover plate is coated with a 20 Ω/\square indium-tin-oxide transparent electrode and with uniaxially buffed polyimide. Aluminum is evaporated onto one edge of the cover plate to allow a wire to make a good contact to the indium-tin-oxide backplane. The cover plate is affixed to the surface of the chip, at a microscopic distance set by small drops of a mixture of chopped glass fibers and Norland 61 UV-cured optical adhesive deposited on the periphery of the active area of the device. The resulting cavity is filled with Merck E7 in the isotropic phase. The mesogenic substance enters the nematic phase as the device slowly cools down.

Figure 2 shows the electro-optic response of a device employing as a lower substrate an integrated circuit fabricated in the Orbit 2.0- μm analog n -well MOSIS complementary metal-oxide-semiconductor process (curves labeled HAN-on-VLSI). The cell gap is 5 μm , and the cavity is filled with Merck E7. Crossed polarizers were used. The response of an area containing approximately six externally driven pixels was measured. Figure 3 shows rows of pixels at maximum and minimum reflection settings. The total phase retardation of the undriven device, 11.4 rad, is within 7.6% of the value predicted by

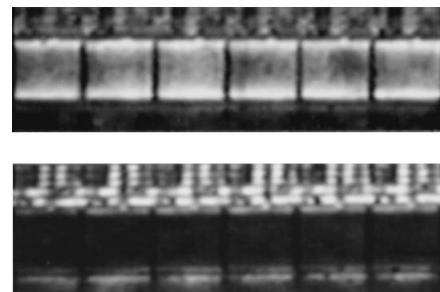


Fig. 3. Rows of six pixels at maximum (top) and minimum (bottom) reflection settings. Voltage-dependent reflectance is also observed in the areas surrounding the pixels, as a result of the presence of conductors at various potentials and depths within the silicon dioxide.

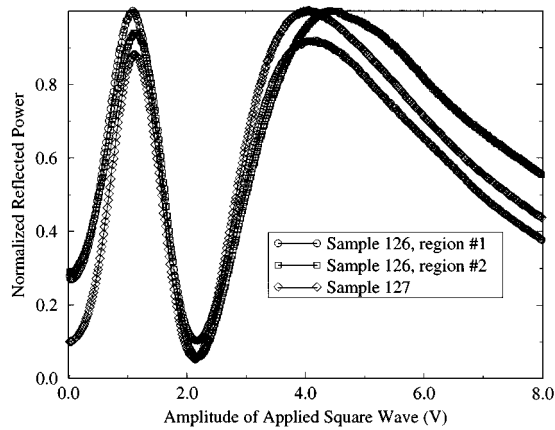


Fig. 4. Electro-optic responses of different areas of the same device (sample 126) and of another device processed by the same procedure (sample 127). Note the excellent uniformity of the voltages corresponding to the first reflectance maximum and minimum.

relation (2), where d was set to $10\ \mu\text{m}$ to account for the two passes of the beam through the modulator. Note that the entire amplitude-modulation range is spanned by application of voltages less than 2.2 V across the modulator electrodes. One of the reasons why the required voltage is higher than in the case of the device with glass substrates is the voltage drop across the protective overcoat (Fig. 1). Imaged contrast ratios in excess of 18:1 have been obtained in HAN-on-VLSI prototypes, without any planarization treatment on the die. The first level of metalization was employed to form the pixel electrodes, since the second-level metal of the Orbit 2.0- μm processes is known to have a poorer surface quality.

Figure 4 shows the electro-optic responses of widely separated areas of the same device (sample 126) and of another device (sample 127) prepared by the same procedure. Note that the voltages corresponding to the first reflectance maximum and minimum of the three curves are very close (within approximately 30 mV). This is an indication of the reliability and uniformity of the process.

The rise and fall times of the HAN-on-VLSI device whose electro-optic response is shown in Fig. 2, with $V_{\text{on}} = 4.42\ \text{V}$ and $V_{\text{off}} = 2.17\ \text{V}$, were 12 and 24.6 ms, respectively. Note that this allows the device to perform video-rate (30-Hz) modulation. If lower driving voltages are desired, the reflectance maximum at 1.12 V can be employed instead of that at 4.42 V; the resulting switching time then increases to 40 ms.

In conclusion, the hybrid alignment method that we described permits nematic liquid crystals, which are used in practically all display applications, to

be efficiently interfaced to silicon VLSI circuitry. The devices are capable of true gray-scale or analog phase modulation at low voltages. For information-processing applications, their lower speed, compared with those of distorted helix ferroelectric and electroclinic modulators, is offset by the low cost, maturity, and ease of use of nematic liquid crystals. Nematics are easier to align than distorted helix ferroelectric materials and avoid the high voltage requirements and the problems related to low tilt angles that are common in electroclinic modulators. HAN-on-VLSI devices are ideally suited, for example, to optical neuromorphic systems processing external stimuli occurring on millisecond time scales (e.g., sensory processing) and to volume holographic memories limited by the response time of the holographic medium. Other applications include analog spatial light modulators, smart pixel arrays, and programmable diffractive elements.

This work was supported by the Advanced Research Projects Agency and the National Science Foundation Center for Neuromorphic Systems Engineering at the California Institute of Technology. J.-J. P. Drolet acknowledges support from the National Sciences and Engineering Research Council of Canada. The authors express their gratitude to Y. Liu for her technical assistance.

*Present address, Department of Physics, The Pennsylvania State University, 215 Davey Laboratory, University Park, Pennsylvania 16802-6301.

References

1. K. M. Johnson, D. J. McKnight, and I. Underwood, *IEEE J. Quantum Electron.* **29**, 699 (1993).
2. I. Underwood, D. G. Vaas, A. O'Hara, D. C. Burns, P. W. McOwan, and J. Gourlay, *Appl. Opt.* **33**, 2768 (1994).
3. D. J. McKnight, D. G. Vass, and R. M. Sillitto, *Appl. Opt.* **28**, 4757 (1989).
4. N. A. Clark and S. T. Lagerwall, *Appl. Phys. Lett.* **36**, 899 (1980).
5. L. K. Cotter, T. J. Drabik, R. J. Dillon, and M. A. Handschy, *Opt. Lett.* **15**, 291 (1990).
6. T. J. Drabik and M. A. Handschy, *Appl. Opt.* **29**, 5220 (1990).
7. D. A. Jared and K. M. Johnson, *Opt. Lett.* **16**, 967 (1991).
8. D. J. McKnight, K. M. Johnson, and R. A. Serati, *Appl. Opt.* **33**, 2775 (1994).
9. R. Barberi and G. Barbero, in *Physics of Liquid Crystalline Materials*, I.-C. Khoo and F. Simoni, eds. (Gordon & Breach, New York, 1988), Chap. IX.
10. "Liquid crystal mixtures for electro-optic displays" (E. Merck, Industrial Chemical Division, September 1992).
11. *MOSIS User Guide*, release 3.1 ed. (MOSIS, Information Sciences Institute, University of Southern California, Marina del Ray, Calif., August 1992).